International Telecommunication Union

ITU-R

Radiocommunication Sector of ITU

Report ITU-R RS.2490-0

(09/2021)

Global survey of radio frequency interference observed by the Aquarius scatterometer in the 1 215-1 300 MHz band and the Aquarius radiometer in the 1 400-1 427 MHz band

RS Series

Remote sensing systems

International Telecommunication Union

Foreword

The role of the Radiocommunication Sector is to ensure the rational, equitable, efficient and economical use of the radio-frequency spectrum by all radiocommunication services, including satellite services, and carry out studies without limit of frequency range on the basis of which Recommendations are adopted.

The regulatory and policy functions of the Radiocommunication Sector are performed by World and Regional Radiocommunication Conferences and Radiocommunication Assemblies supported by Study Groups.

Policy on Intellectual Property Right (IPR)

ITU-R policy on IPR is described in the Common Patent Policy for ITU-T/ITU-R/ISO/IEC referenced in Resolution ITU-R 1. Forms to be used for the submission of patent statements and licensing declarations by patent holders are available from http://www.itu.int/ITU-R/go/patents/en where the Guidelines for Implementation of the Common Patent Policy for ITU-T/ITU-R/ISO/IEC and the ITU-R patent information database can also be found.

Series of ITU-R Reports

(Also available online at http://www.itu.int/publ/R-REP/en)

Series	Title
BO	Satellite delivery
BR	Recording for production, archival and play-out; film for television
BS	Broadcasting service (sound)
BT	Broadcasting service (television)
F	Fixed service
M	Mobile, radiodetermination, amateur and related satellite services
P	Radiowave propagation
RA	Radio astronomy
RS	**Remote sensing systems**
S	Fixed-satellite service
SA	Space applications and meteorology
SF	Frequency sharing and coordination between fixed-satellite and fixed service systems
SM	Spectrum management

Note*: This ITU-R Report was approved in English by the Study Group under the procedure detailed in Resolution ITU-R 1.*

Electronic Publication
Geneva, 2021

REPORT ITU-R RS.2490-0

Global survey of radio frequency interference observed by the Aquarius scatterometer in the 1 215-1 300 MHz band and the Aquarius radiometer in the 1 400-1 427 MHz band

(Question ITU-R 255/7)

(2021)

TABLE OF CONTENTS

Page

Scope

This Report presents global surveys of radio frequency interference (RFI) levels that were observed by Aquarius L-band sensors in the Earth exploration-satellite service (EESS) (active) frequency band 1 215-1 300 MHz and the EESS (passive) frequency band 1 400-1 427 MHz during the 2013 to 2015 time period. It should be noted that the Aquarius mission successfully completed its operations in June 2015. It must be noted that observations in these frequency bands have been, and will continue to be, important for studies including, but not limited to, meteorology, land and water management, and climate change. Therefore, future missions utilizing these frequency bands are expected. The determination of future mission objectives relies on information concerning the interference environment that these missions would encounter. This Report provides information that may be taken into account when planning future mission objectives in these frequency bands.

This Report is intended to assist EESS operators in their mission planning and its contents are not intended to prompt any future conference actions or changes to the Radio Regulations (RR).

1 Introduction

This Report presents global surveys of RFI levels that were observed by the Aquarius scatterometer in the Earth exploration-satellite service (EESS) (active) frequency band 1 215-1 300 MHz and Aquarius radiometer in the EESS (passive) frequency band 1 400-1 427 MHz during the 2013 to 2015 time period.

The frequency band 1 215-1 300 MHz is allocated on a primary basis to the radionavigation-satellite service (RNSS) and radiolocation service (RLS), and the band 1 240-1 300 MHz is also allocated on a primary basis to the aeronautical radionavigation service (ARNS). Systems operating under the EESS (active) in the frequency band 1 215-1 260 MHz cannot claim protection from systems operating in the RLS or ARNS, and other services allocated on a primary basis (see RR No. **5.332**). Emissions from the terrestrial radars operating in the RLS and ARNS are radio frequency interferences (RFI) to the EESS (active) sensors in the sense that their emissions can degrade the performance of the EESS (active) sensors. However, it is recognized that the EESS (active) sensors operating in this frequency band have to accept the RLS and ARNS emissions in accordance with the provisions of RR No. **5.332**.

The EESS (passive) frequency band 1 400-1 427 MHz is allocated solely for passive operations. The adjacent bands are allocated to the fixed, mobile and radio location services. Excessive unwanted emissions in the passive frequency band originating from the active services in adjacent bands, and unauthorised emissions occurring within the passive frequency band can impact the passive sensors operating in this passive frequency band and identified as RFI to these passive sensors. However, it is recognized that unwanted emissions from services in the adjacent bands may be in accordance with the provisions of Resolution **750 (Rev.WRC-19)**.

This Report provides a seven-day global map of RFI power observed by the Aquarius scatterometer around 1 260 MHz during the 2013 to 2015 period. Presented for comparison is the RF environment observed by the Aquarius radiometer in the 1 400-1 427 GHz frequency band in a seven-day global map of brightness temperature obtained during the same seven-day period as was observed by the scatterometer. The RFI as measured by these two spaceborne active/passive sensors is also described to the extent possible. This information is provided to assist in the design of future spaceborne active/passive sensors in these bands.

2 Related ITU-R Recommendations and Reports

The following ITU-R Recommendations and Reports are related to this Report on the Radio Frequency Interference (RFI) observed by the Aquarius scatterometer and radiometer:

– Recommendation ITU-R RS.1166-4 – Performance and interference criteria for active spaceborne sensors

– Recommendation ITU-R RS.1859-1 – Use of remote sensing systems for data collections to be used in the event of natural disasters and similar emergencies

– Recommendation ITU-R RS.1883-1 – Use of remote sensing systems in the study of climate change and the effects thereof

– Recommendation ITU-R RS.2017-0 – Performance and interference criteria for satellite passive remote sensing

– Recommendation ITU-R RS.2106-0 – Detection and resolution of radio frequency interference to Earth exploration-satellite service (passive) sensors

– Report ITU-R RS.2491-0 – Global survey of radio frequency interference observed by the SMAP radar in 1 215-1 300 MHz band and SMAP radiometer in the 1 400-1 427 MHz band

– Report ITU-R RS.2492-0 – Global survey of radio frequency interference observed by SMOS radiometer in the EESS (passive) band 1 400-1 427 MHz

– Report ITU-R RS.2178-0 – The essential role and global importance of radio spectrum use for Earth observations and for related applications

– Report ITU-R RS.2311-0 – Pulsed radio frequency signal impact measurements and possible mitigation techniques between Earth exploration-satellite (active) systems and RNSS systems and networks in the band 1 215-1 300 MHz.

3 List of acronyms and abbreviations

ADC Analogue digital converter

ARNS Aeronautical radionavigation service

BSS Broadcasting satellite system

BT Brightness temperature

CCDF Complementary cumulative distribution function

CDF Cumulative distribution function

CNES Centre national d’études spatiales

EESS Earth exploration-satellite service

RFI Radio-frequency interference

RR Radio Regulations

SMAP Soil moisture active passive

SMOS Soil moisture ocean salinity

WRC World Radiocommunication Conference

4 Regulatory situation in the 1 215-1 300 MHz and 1 400-1 427 MHz frequency bands

4.1 Regulatory situation in the 1 215-1 300 MHz frequency band

The 1 215-1 300 MHz frequency band is allocated on a primary basis to the EESS (active) with constraints given in ITU-R Radio Regulations (RR) No. **5.332** in the 1 215-1 260 MHz sub-band, Nos. **5.332** and **5.335** in the 1 240-1 300 MHz sub-band and No. **5.335A** in the 1 260-1 300 MHz sub-band. Radio Regulations No. **5.332** states that "In the band 1 215-1 260 MHz, active spaceborne sensors in the Earth exploration-satellite and space research services shall not cause harmful interference to, claim protection from, or otherwise impose constraints on operation or development of the radiolocation service, the radionavigation-satellite service and other services allocated on a primary basis." Radio Regulations No. **5.335** states that "In Canada and the United States in the band 1 240-1 300 MHz, active spaceborne sensors in the Earth exploration-satellite and space research services shall not cause interference to, claim protection from, or otherwise impose constraints on operation or development of the aeronautical radionavigation service."

Radio Regulations No. **5.335A** states that "In the band 1 260-1 300 MHz, active spaceborne sensors in the Earth exploration-satellite and space research services shall not cause harmful interference to, claim protection from, or otherwise impose constraints on operation or development of the radiolocation service and other services allocated by footnotes on a primary basis."

Since EESS (active) cannot claim protection from the radiolocation service, the aeronautical radionavigation service nor the radionavigation-satellite service in these respective sub-bands, EESS (active) systems have to accept the RFI received from these other primary services.

Figure 1 shows the ITU-R frequency allocations in and around the 1 215-1 300 MHz frequency range.

FIGURE 1

ITU-R frequency allocations in the 1 215-1 300 MHz range and adjacent frequency bands

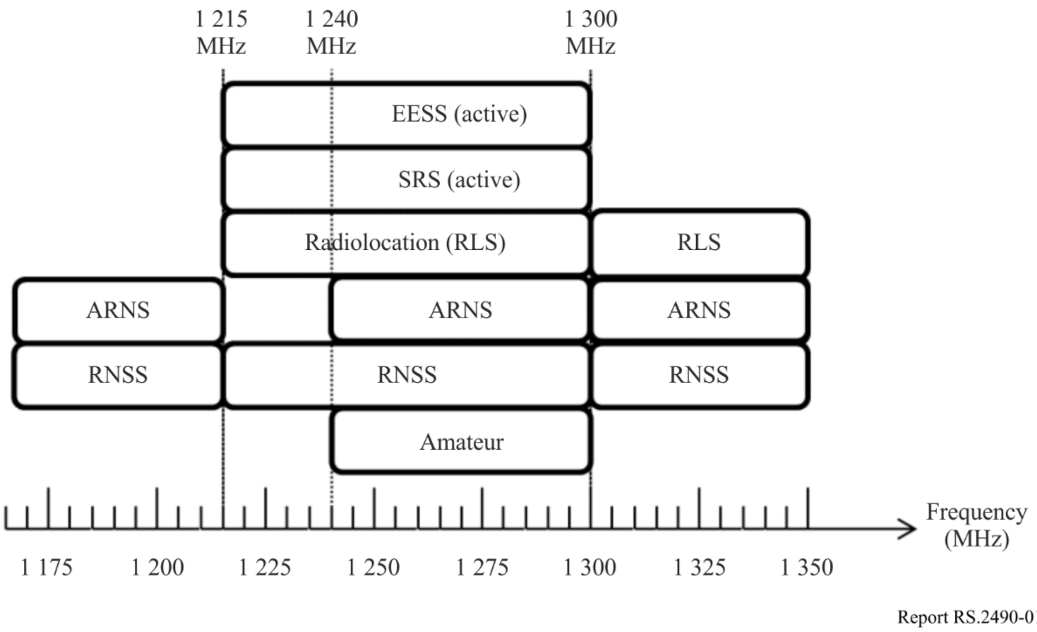

Below the 1 215-1 300 MHz band allocated to EESS (active) is the 1 164-1 215 MHz band, which is allocated on a primary basis to the ARNS and the RNSS (space-to-Earth) (space-to-space).

Above the 1 215-1 300 MHz band is the 1 300-1 350 MHz band, which is allocated on a primary basis to the RLS, the ARNS and the RNSS (Earth-to-space).

4.2 Regulatory situation in the 1 400-1 427 MHz frequency band

The band 1 400-1 427 MHz is allocated on a primary basis to the EESS (passive), SRS (passive) and to the radio astronomy service as shown in Fig. 2. All emissions are prohibited in this band according to RR No. **5.340**. In addition, WRC-07 adopted Resolution **750** on the compatibility between the EESS (passive) and relevant active services. Concerning the 1 400-1 427 MHz band, Resolution **750 (Rev.WRC-19)** contains the mandatory and recommended maximum levels of unwanted emissions from active service stations within the EESS (passive) band applicable to the ITU-R services allocated in the adjacent bands.

FIGURE 2

ITU-R frequency allocations in the 1 400-1 427 MHz range and adjacent frequency bands

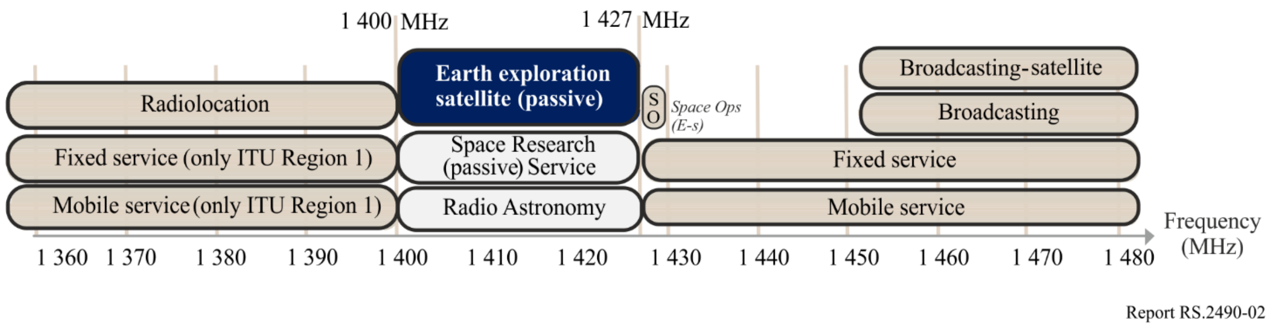

The Aquarius mission obtained accurate global observations of emissions originating from land and ocean surfaces since the atmosphere is almost transparent in the 1 400-1 427 MHz frequency band. In addition, the sensitivity to varying emissivity resulting from changes of the water content in the soil and the salinity in the oceans is high for lower microwave frequencies in comparison to the measurements obtained at higher frequencies by operational sensors. The all-weather-all-surfaces capabilities of the 1 400-1 427 MHz frequency band addresses the needs of a large range of user communities and applications.

The following sections describe the RFI as measured during the 2013 to 2015 period by the Aquarius mission spaceborne active and passive sensors which were operating entirely within their allocated EESS frequency bands of 1 215-1 300 MHz and 1 400-1 427 MHz. Section 2 presents the RFI scenario, which was detected by the radar scatterometer of the Aquarius mission. Section 3 presents the RFI scenario which was detected by the radiometer of the Aquarius mission.

The information provided in this Report may be taken into account during the design of future spaceborne sensors in which are intended to operate in the 1 215-1 300 MHz and 1 400-1 427 MHz frequency bands.

5 RFI as observed by the Aquarius scatterometer

5.1 Description of Aquarius scatterometer

Aquarius was a microwave remote sensing instrument designed to obtain global maps of the surface salinity field of the oceans from space and was flown on the Aquarius/Satélite de Aplicaciones Científicas-D (SAC-D) mission, a partnership between the USA National Aeronautics and Space

Administration (NASA) and Argentina Comisión Nacional de Actividades Espaciales (CONAE). Aquarius was successfully launched in June 2011. The mission ended in June 2015.

The Aquarius instrument was a combination of scatterometer and radiometer operating at the centre frequencies of 1.26 GHz for the scatterometer (active sensor) and at 1.413 GHz for the radiometer (passive sensor). The primary instrument for measuring salinity was the radiometer which responds to salinity because of the modulation salinity produces on thermal emission from sea water. The scatterometer provided a correction for surface roughness (waves) which is one of the greatest unknowns in the retrieval.

The Aquarius scatterometer mapped the surface of the Earth every seven days. The Aquarius scatterometer was a total power scatterometer operating at a center frequency of 1.26 GHz and was designed to acquire radar backscatter signals that were used to estimate ocean-surface roughness. The Aquarius scatterometer, co-pointed with the primary radiometer subsystem, obtained this data to provide brightness temperature corrections to the salinity measurement performed by the radiometer.

The radar scatterometer collected fully polarimetric returns which were summed to represent the total ocean backscatter. The linearly frequency modulated (FM) pulses had a pulse duration of 1 ms and a range bandwidth of 4 MHz. Three beams from an offset –parabolic reflector provided a 280 km width swath. The 2.9 m × 2.5 m offset parabolic reflector with three feeds produced inner, middle and outer 3 dB beam widths of 6.5, 6.7 and 7.1 degrees, respectively.

An illustration of the three beams of the Aquarius scatterometer and the three footprints on the Earth is shown in Fig. 3. Each of the three beams was pointed at different off-set nadir angles in order for the footprints to cover 390 km across track on the ground. The radar cycled among the three beams every 60 milliseconds.

FIGURE 3

Illustration of three footprints of three antenna beams of Aquarius scatterometer

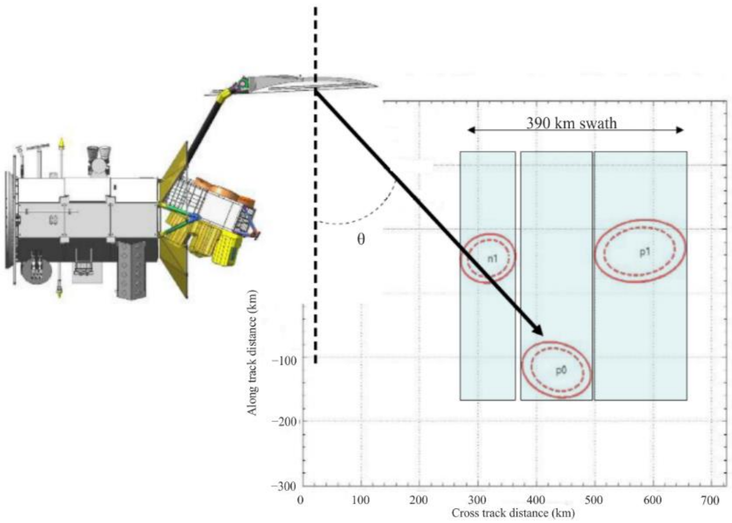

Report RS.2490-03

5.2 RFI detection

For the Aquarius scatterometer, an onboard radio frequency interference (RFI) detection scheme was implemented to flag RFI prior to further ground processing. Onboard RFI flagging is not sufficient for removing RFI effects for further processing. An RFI detection and filtering algorithm was developed for ground data processing that has enabled the effective removal of most RFI over the ocean, and substantial removal over most land areas. Certain land areas remain pathologically contaminated with RFI, however.

The onboard RFI detection algorithm is a user-adjustable, PDF thresholding algorithm operating at the level of the high-rate 16 MHz digital sampling. The default thresholds were set to detect a common ATC radar pulse type with negligible false-positive detections, but shorter length or lower-power pulses are missed. Integrated over the ~2 ms receive windows, even these latter types of pulses could be significant RFI sources. In addition, the onboard flagging scheme can only operate during noise-only pulses, as the natural radar echoes would usually trigger the RFI flag. For RFI that appears only in echoes and not in the adjacent noise-only detection windows, these RFI sources would not be flagged at all by the onboard algorithm.

An additional RFI detection and removal step implemented in the ground processing consists of a two-pass median filter and outlier detection routine. Data values which depart from the median values by more than a specified number of standard deviations are flagged as RFI and removed from further data averaging. Where RFI is ubiquitous, the RFI-tainted values are used in the data averaging with a data quality flag indicating this. The resulting scatterometer echo power data, cleaned of RFI using both detection schemes, appears to be free of RFI over most of the oceans. As an example, for a one-week sample of beam 3H data, the percentage of no data flagged as RFI-contaminated was shown to be 73.7%, 84.3% and 64.8% globally, over land areas, and over ocean areas, respectively. and globally averaged for a one-week sample of beam 3H data. This leaves 26.3%, 15.7% and 35.3% globally, over land areas, and over ocean areas, respectively, of data flagged as RFI-contaminated (combination of little RFI, much RFI, and all RFI). The amount of RFI remaining can be independently verified by examining the density of negative backscatter power and looking at the ocean cross-pol power levels.

5.3 Types of maps

The Aquarius scatterometer radar operates with a pulse sequence consisting of alternating horizontal (H) and vertical (V) transmit and receive polarizations, along with intervening noise-only measurements on each polarization. We thus have echo data with HH, VV, HV, and VH transmit-receive polarizations, and nH and nV noise-only receive polarizations. During every other nV measurement, a noise diode (CND) injects a signal into the receive path for the Aquarius radiometer; this CND signal raises the apparent nV noise floor and usually triggers our onboard RFI flag. This CND effect needs to be accounted for in any RFI detection and mitigation scheme.

Several types of maps are used in this Report:

– Global RFI maps: global RFI maps show the ADC input power in the nH and nV channels over the world with a seven-day global mapping period as shown in Fig. 4.

– Regional RFI maps: regional RFI maps (Regions 1, 2 and 3) with a quarter of a year mapping period show the ADC input power for select CDF values; Figure 6 shows the noise power for CDF value 99.9 % in Region 1 observations in the first quarter of year 2014.

5.4 Types of RFI sources

The spatial and temporal resolution of the Aquarius scatterometer data permit the determination of individual RFI sources and comparisons of the predicted RFI effects with those actually observed. RFI maps show examples of identifying the locations of Aquarius RFI hot-spots with nearby ATC radars over North America. It is also possible to compare the expected RFI signals generated from RFI and source/receiver modelling to the RFI levels Aquarius actually observes.

Figure 4 is a map of the H-pol noise-only receive channel over a seven-day global mapping period. There are hot regions of RFI in eastern North America, Europe, and East Asia, with numerous RFI hot spots in other land areas. Close inspection of maps like these and individual radar time series reveals two types of RFI: that due to a) the main beam of a ground radar entering the sidelobes of the Aquarius scatterometer, and b) ground radar sidelobes entering one of the Aquarius radar main beams. Type (a) RFI can be apparent as far as 3 000 km from the RFI source and well into the nearby oceans and usually appears simultaneously in all three radar beams (e.g. the "halos" about the continents in Fig. 4). Type (b) appears at the location of the RFI source and usually manifests in only one of the three beams at one time (e.g. the continental "hot spots" in Fig. 4).

5.5 Historical observation of RFI by the Aquarius scatterometer at 1 260 MHz

The Aquarius scatterometer radar alternated horizontal (H) and vertical (V) transmit and receive polarized pulses, and interleaved noise-only measurements on each polarization. The echo data had HH, VV, HV, and VH transmit-receive polarizations, and noise horizontal (nH) and nV noise-only receive polarizations. During every other nV measurement, a noise diode injected a signal into the receive path which raised the apparent nV noise floor.

FIGURE 4

Aquarius scatterometer global RFI maps

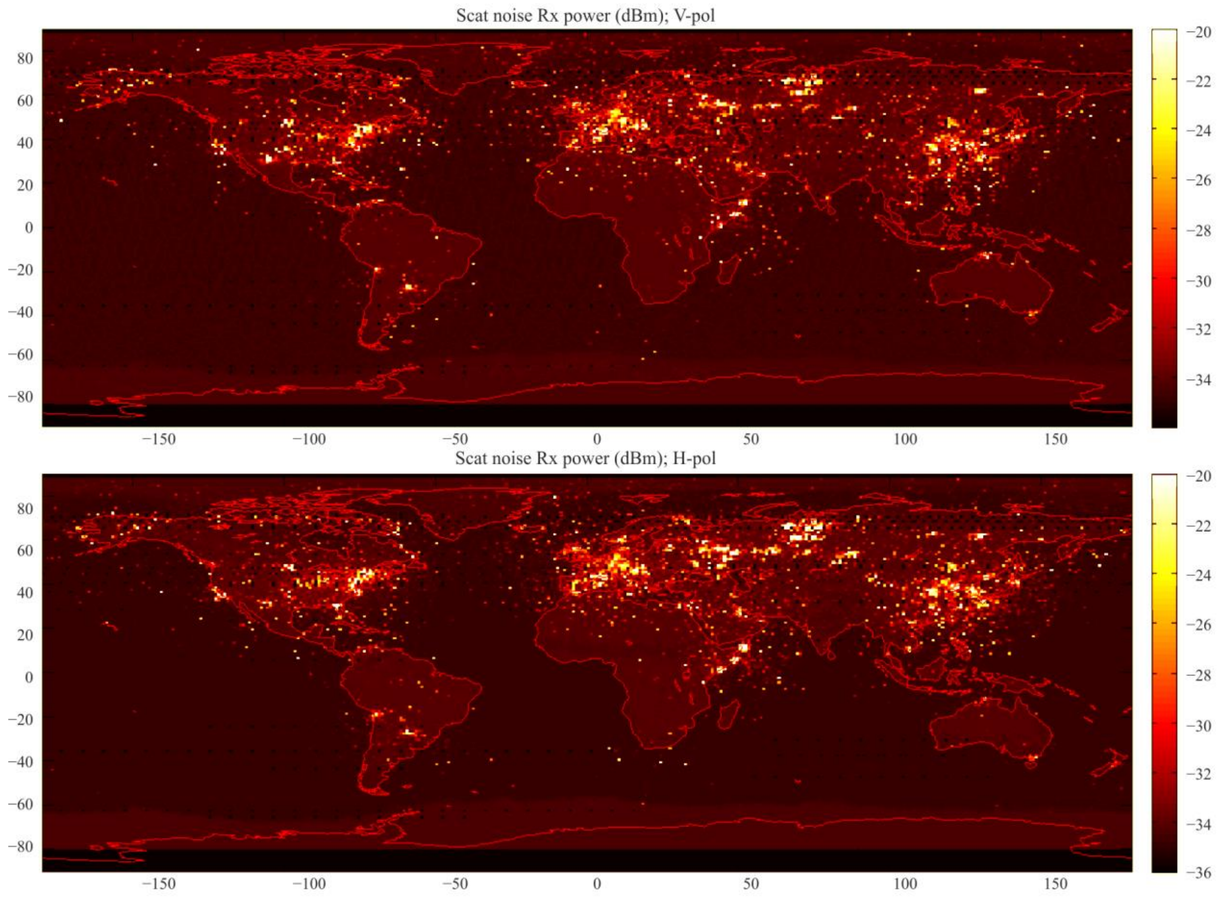

Report RS.2490-04

Figure 5 shows the timing sequence of the Aquarius instrument.

Following the June 2011 launch and activation of the Aquarius instrument, RFI was observed to be present in the Aquarius scatterometer band 1 258-1 262 MHz, particularly over Japan and China.

Individual RFI sources were identified from the Aquarius scatterometer RFI data using the spatial and temporal resolution. The observed RFI effects were compared with the predicted RFI effects.

Figure 6 shows a complementary cumulative distribution curve (1-CDF) of RFI levels as observed during the January to March 2013 time period and the update during the January to March 2015 time period for the continental U.S. The receiver gain from the antenna feeds to the ADC input was about 67 dB, so for example if the RFI level were -10 dBm at the ADC input, then the signal level at the antenna feeds was −76 dBm or −106 dBW.

Figures 7 and 8 show the RFI maps of the observed noise for CDF value 99.9% in Region 1 for observations in the first quarter of year 2014 and in the first quarter of year 2015, respectively.

Figures 9 and 10 show the RFI maps of the observed noise for CDF value 99.9% in Region 2 for observations in the first quarter of year 2014 and in the first quarter of year 2015, respectively.

Figures 11 and 12 show the RFI maps of the observed noise for CDF value 99.9% in Region 3 for observations in the first quarter of year 2014 and in the first quarter of year 2015, respectively.

The expected RFI signal levels generated from RFI and source/receiver modeling were compared to the RFI levels that Aquarius actually observed. The RFI levels into the Aquarius scatterometer from the ground radars were estimated using modelled characteristics of known emitters in the US and Canada for long-range tracking radars. The 1-CDF curve of modelled RFI compared favourably with the 1-CDF curved of observed RFI over North America.

FIGURE 5

Timing sequence of Aquarius instrument

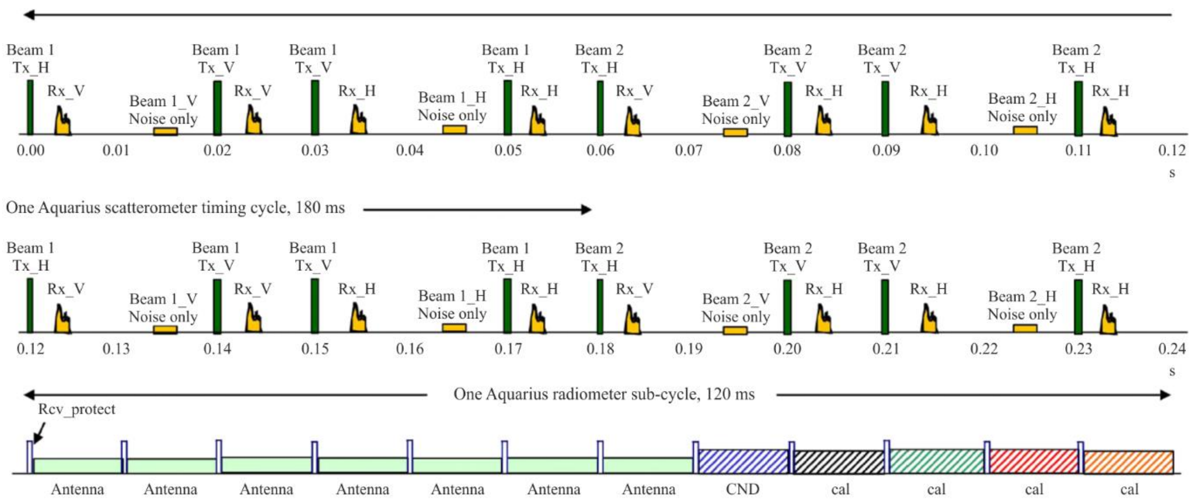

Report RS.2490-05

FIGURE 6

1-CDF Distribution of observed noise power at scatterometer ADC input for North America during Jan-Mar 2013 (left) and Jan-Mar 2015 (right)

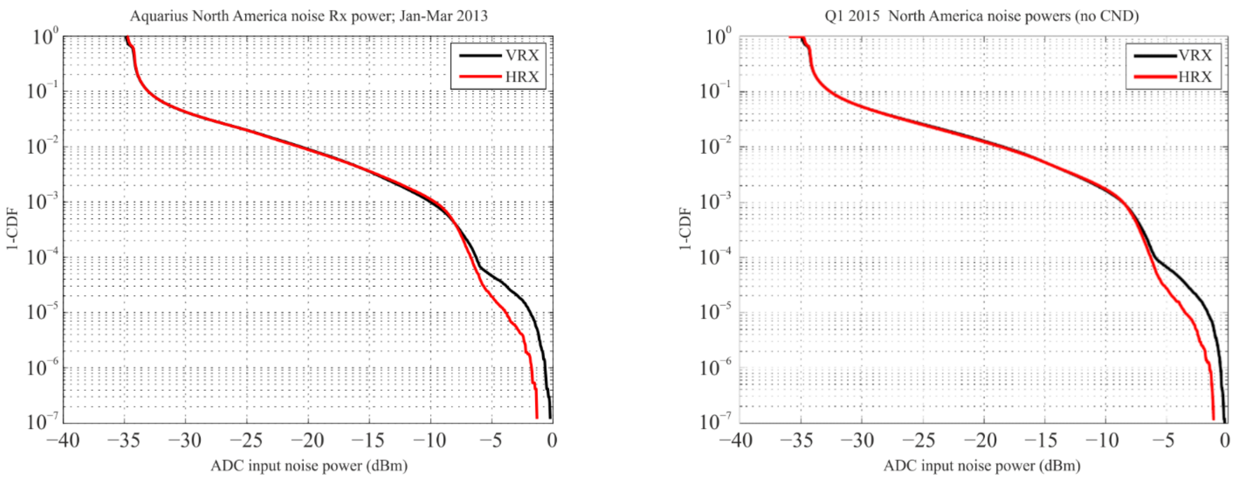

Report RS.2490-06

FIGURE 7

Map of observed noise power (99.9%) at Aquarius scatterometer ADC input for Europe and Northern Africa (Region 1) (1st quarter of year 2014)

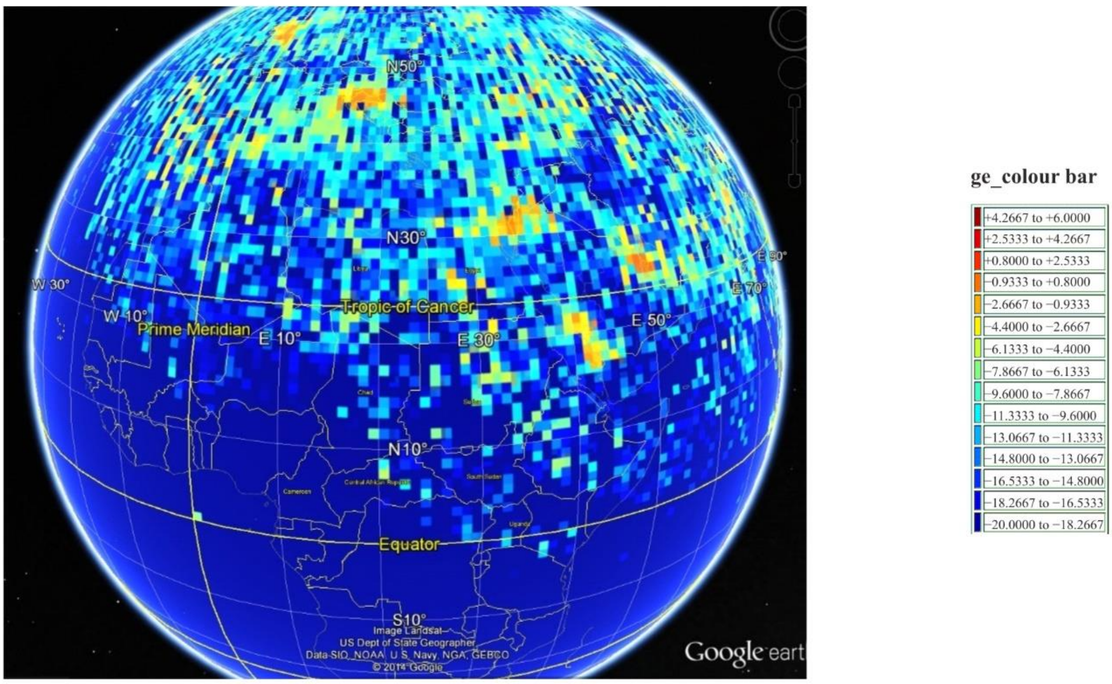

Report RS.2490-07

FIGURE 8

Map of observed noise power (99.9%) at Aquarius scatterometer ADC input for Europe and Northern Africa (Region 1) (1st quarter of year 2015)

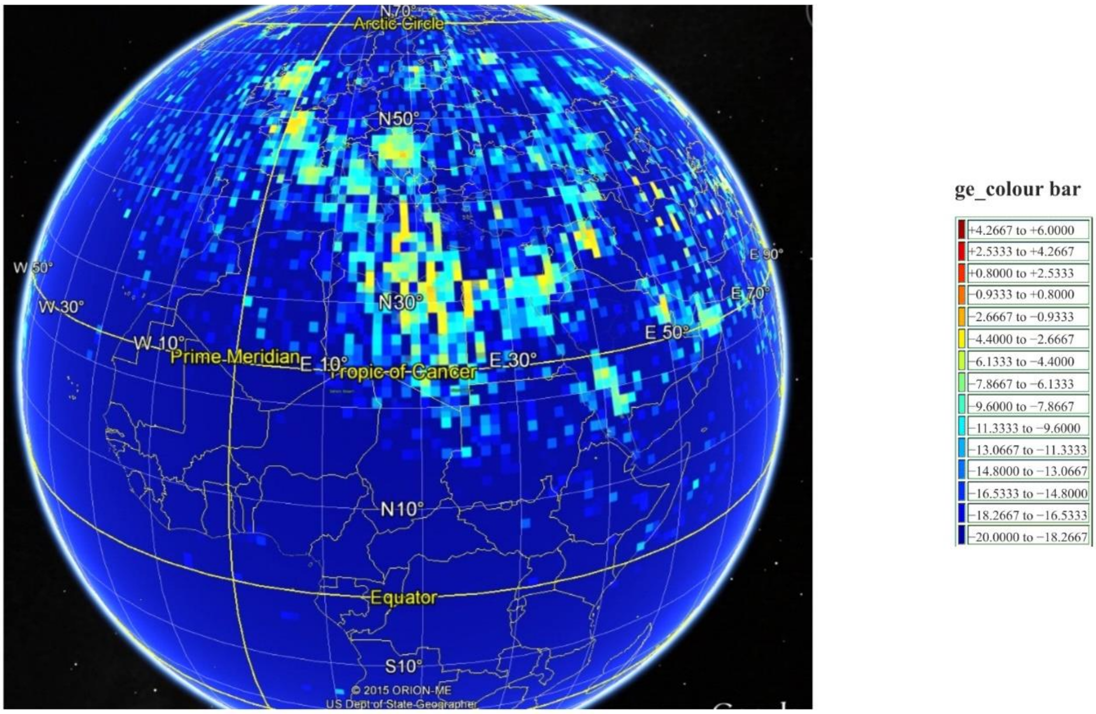

Report RS.2490-08

FIGURE 9

Map of observed noise power (99.9%) at Aquarius scatterometer ADC input for North America (Region 2) (1st quarter of year 2014)

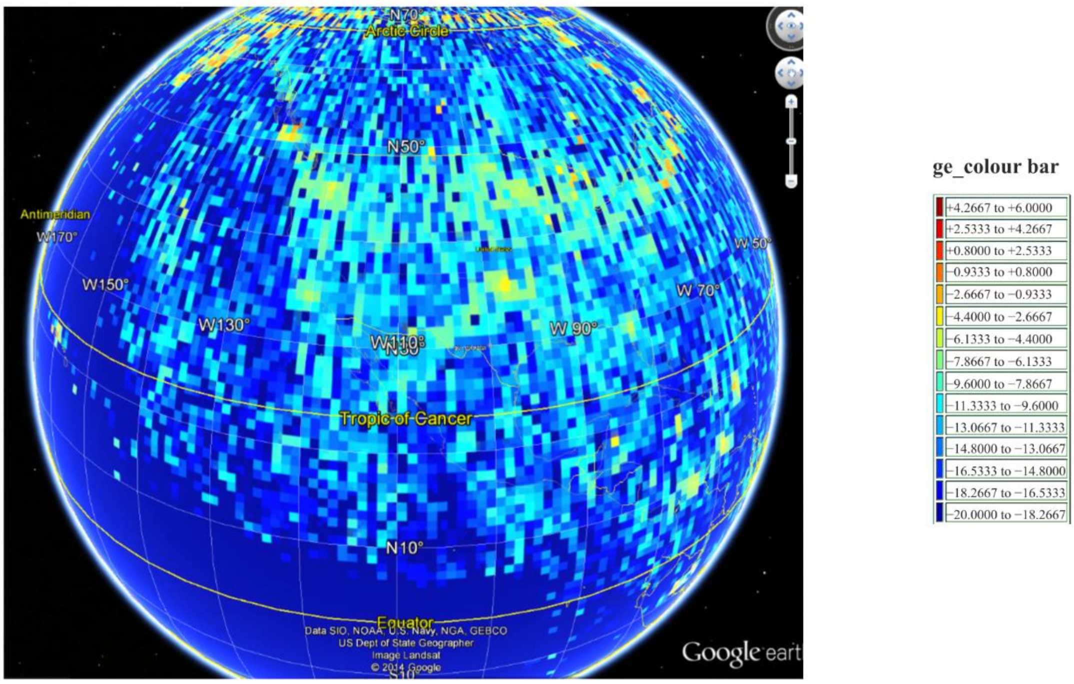

Report RS.2490-09

FIGURE 10

Map of observed noise power (99.9%) at Aquarius scatterometer ADC input for North America (Region 2) (1st quarter of year 2015)

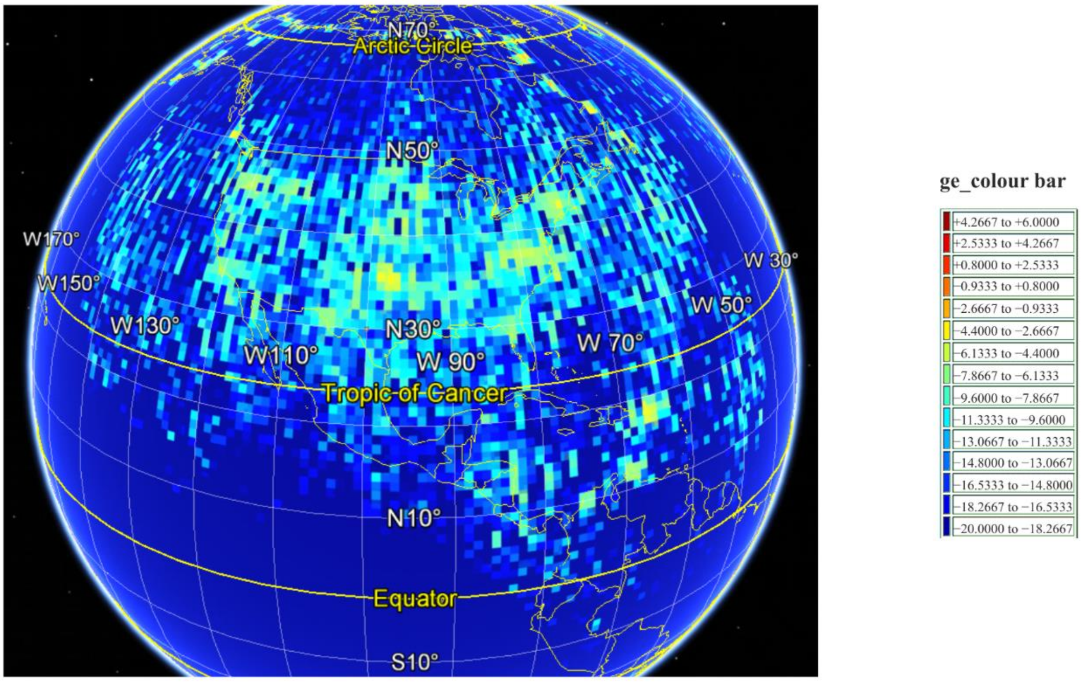

Report RS.2490-10

FIGURE 11

Map of observed noise power (99.9%) at Aquarius scatterometer ADC input for Asia (Region 3) (1st quarter of year 2014)

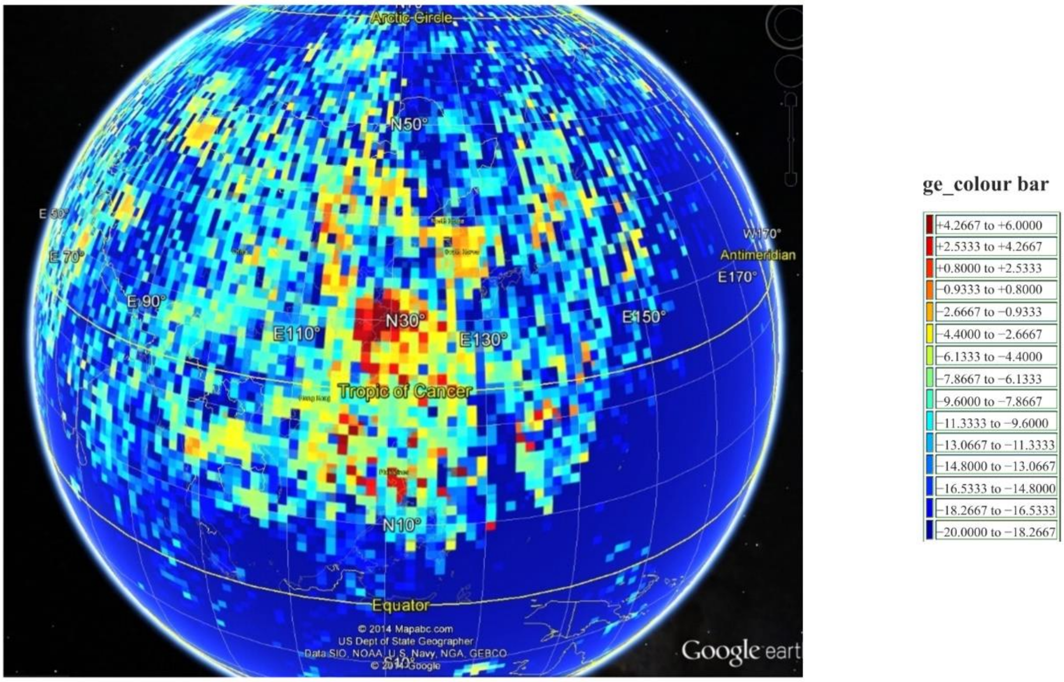

Report RS.2490-11

FIGURE 12

Map of observed noise power (99.9%) at Aquarius scatterometer ADC input for Asia (Region 3) (1st quarter of year 2015)

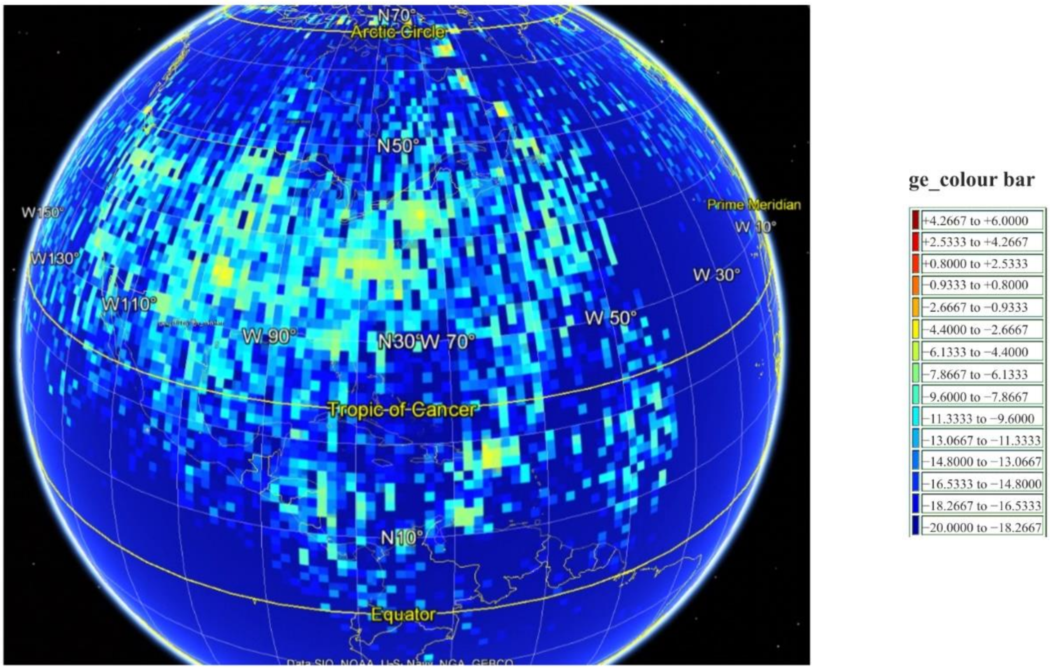

Report RS.2490-12

As with the scatterometer which shared the antennas with the radiometer, the three beams from an offset parabolic reflector provided a 390 km width swath. The 2.9 m × 2.5 m offset parabolic reflector with three feeds produced inner, middle and outer 3 dB beam widths of 6.1, 6.2 and 6.4 degrees, respectively. There are three radiometers, one for each of the feeds (beams). The radiometers are fully polarimetric. The radiometers make measurements at horizontal polarization, vertical polarization and at ±45 degrees. The third Stokes parameter, obtained from the measurement at ±45 degrees was used to derive a correction for Faraday rotation. Oversampling of the radiometer measurements provides short subsamples which are averaged together to reduce radiometric noise. When RFI is detected in some of the subsamples, they are removed from the average in ground processing. Oversampling is believed to be especially helpful for overcoming pulsed RFI such as are produced by large air traffic control and early warning radars. Ground processing of the Aquarius radiometric data detects the presence of RFI by examining the variance of the subsamples and flagging those which deviate from their neighbors more than can be confidently explained by normal radiometric noise statistics.

6 RFI as observed by the Aquarius radiometer

6.1 Description of Aquarius radiometer

The Aquarius radiometer returned brightness measurements over most of the Earth, including land and ice as well as ocean areas. As far as timing for the hardware, the fundamental timing unit was 10 ms (approximately 1 ms for the scatterometer transmit pulse and 9 ms of observation time for the radiometer). The radiometer and scatterometer operations were alternated so that the two sensors looked at the same piece of ocean nearly simultaneously. The three radiometers (one for each beam) operated in parallel. During 120 ms, each radiometer collected seven samples (9 ms long and repeated each 10 ms) looking into the antenna followed by five samples devoted to the calibration sources (two noise diodes and Dicke load). This 120-ms sequence was then repeated. However, because of limitations with the onboard data storage, the radiometer could not download all of these data. The first and second 10 ms antenna looks were averaged together, as were the third and fourth. The next three antenna looks were left at the 10-ms resolution. The samples of the calibration references transmitted to the ground were the average of ten samples.

6.2 RFI detection

The measurement sampling rate of the Aquarius radiometer is significantly higher than the Nyquist spatial sample rate dictated by its antenna beam width in order to enhance its ability to detect and mitigate anticipated forms of RFI. When RFI is not present, these short subsamples are averaged together to reduce radiometric noise. When RFI is detected in some of the subsamples, they are removed from the average in ground processing. Oversampling in this way is believed to be especially helpful for overcoming pulsed RFI such as are produced by large air traffic control and early warning radars. Ground processing of the Aquarius radiometer data detects the presence of RFI by examining the variance of the subsamples and flagging those which deviate from their neighbors more than can be confidently explained by normal radiometric noise statistics.

6.3 Types of maps

The Aquarius radiometer operates with a pulse sequence with the fundamental timing unit of 10 ms (approximately 1 ms for the scatterometer transmit pulse and 9 ms of observation time for the radiometer). The three radiometers (one for each beam) operated in parallel. During 120 ms, each radiometer collected seven samples (9 ms long and repeated each 10 ms) looking into the antenna followed by five samples devoted to the calibration sources (two noise diodes and Dicke load). This 120 ms sequence was then repeated.

Several types of maps are used in this Report:

– Global RFI maps: global RFI maps show the brightness temperature (BT) in the horizontal and vertical channels over the world with a seven-day global mapping period as shown in Fig. 13.

– Regional RFI maps: regional RFI maps (Regions 1, 2 and 3) with a quarter of a year mapping period show the brightness temperature (BT); Figure 14 shows the BT in Region 1 observations in the first quarter of year 2014.

FIGURE 13

Map of observed BT at radiometer input over the world (seven days in 2011-days 329 to 335)

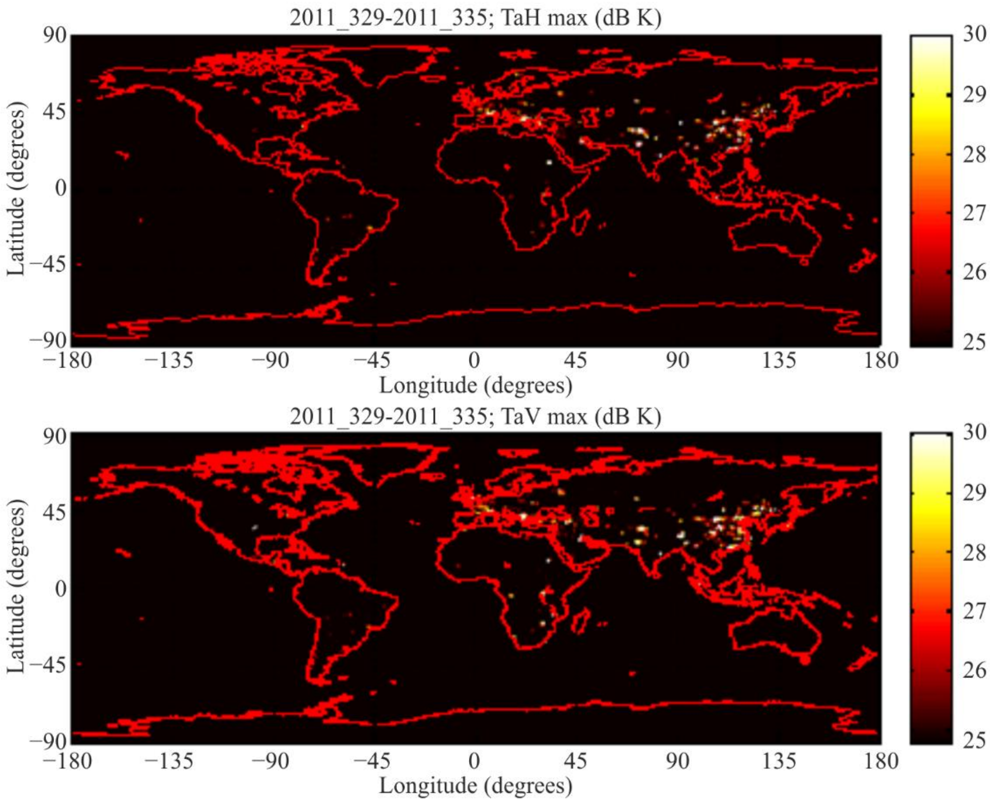

Report RS.2490-13

6.4 Types of RFI sources

The types of RFI sources can be categorized by whether they are in-band or out-of-band and whether they are in the antenna mainlobe or sidelobes:

– In-band emissions in the protected band 1 400-1 427 MHz: These RFI sources in-band are caused by unauthorized sources.

– Out-of-band emissions from adjacent bands: These RFI sources with high emission levels may belong to the radar systems in the adjacent bands.

– Mainlobe antenna sources: These RFI sources in the antenna mainlobe appear typically on land or ocean at the precise location of the land or ocean (shipborne) sources.

– Sidelobe antenna sources: These RFI sources in the antenna sidelobes appear typically in the ocean at locations not where they appear to be in the RFI maps but rather on the land nearby.

6.5 Aquarius radiometer observation of the brightness temperature

The Aquarius radiometer operations were alternated so that the two sensors looked at the same piece of ocean nearly simultaneously as illustrated in Figure 4, which shows the timing sequence of the Aquarius instrument.

The observed radiometer brightness temperature for each 100 km beam footprint is sampled once every seven days. Over the first quarter of years 2013 and 2015, there were about 13 samples of radiometer brightness temperature (BT) per beam footprint over the approximately 90 days from which a histogram and complementary cumulative distribution function (1-CDF or CCDF) of the BT values in dB-K were produced in Fig. 14.

For the following RFI maps in Figs 15 to 20 of the observed maximum BT values in dB-K, the BT values are pseudocolour-coded. The Figures show the BT maps for the first quarter of years 2014 and 2015. The pseudocolour legend in the ‘ge-colourbar’ shows fifteen dB-K bins of values equally distributed over the range of +20 dB-K to +32 dB-K.

Figure 14 shows the complementary CDF plots (1-CDF or CCDF) of the radiometer brightness temperature (BT) in dB K, as observed over North America during the January-to-March 2013 time period (top image) and during the January-to-Mar 2015 time period (bottom image) for the continental U.S.

Figures 15 and 16 show the RFI maps of the observed radiometer maximum brightness temperature (BT) in dB K in Region 1 for observations in the first quarter of year 2014 and in the first quarter of year 2015, respectively. The same colour bar legend is applicable to both Figures, as for the next two pairs of Figures.

Figures 17 and 18 show the RFI maps of the observed radiometer maximum brightness temperature (BT) in dB K in Region 2 for observations in the first quarter of year 2014 and in the first quarter of year 2015, respectively.

Figures 19 and 20 show the RFI maps of the observed radiometer maximum brightness temperature (BT) in dB K in Region 3 for observations in the first quarter of year 2014 and in the first quarter of year 2015, respectively.

The radiometer BT maps show that there were regions of high RFI in eastern North America, Europe, and East Asia, with numerous other high RFI regions in other land areas.

FIGURE 14

CDF distribution of observed BT at radiometer input for North America (Jan-Mar 2013, top) and (Jan-Mar 2015, bottom)

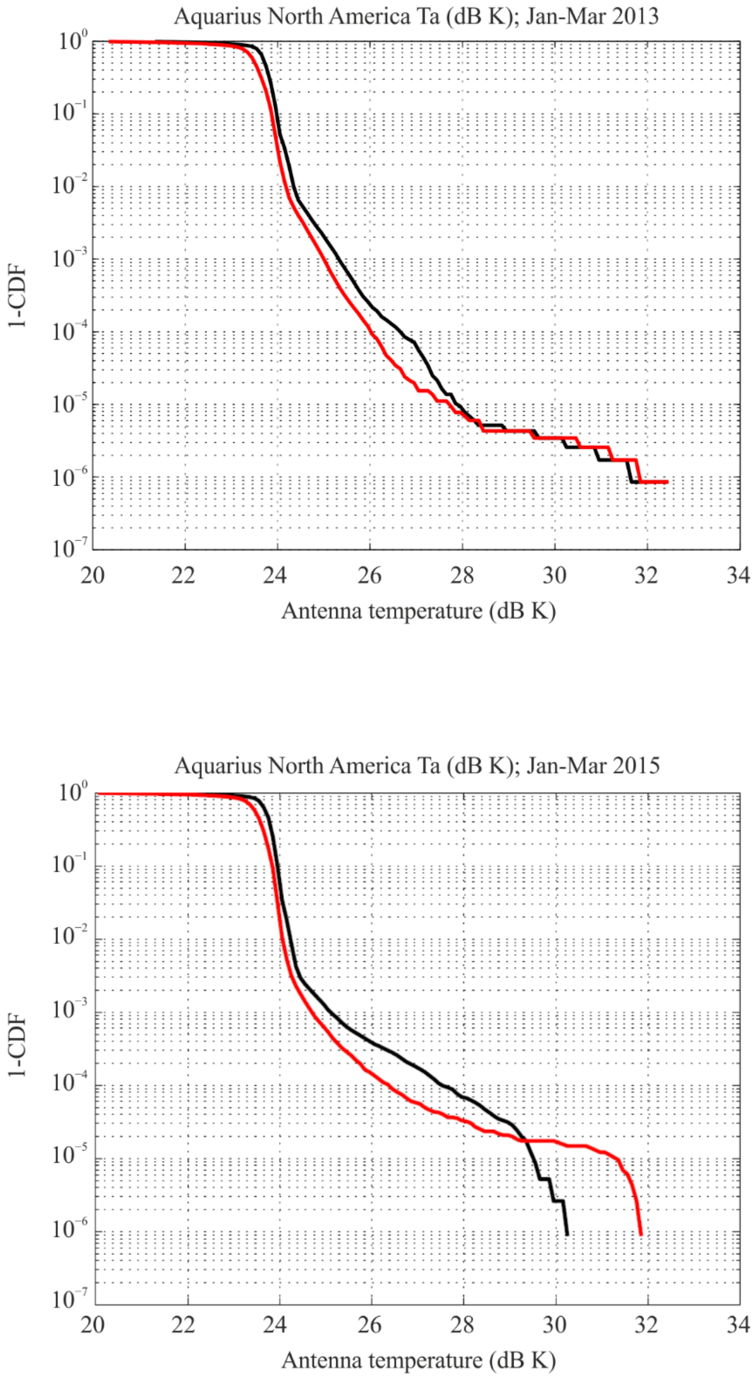

Report RS.2490-14

FIGURE 15

Map of observed BT at radiometer input for Europe and Northern Africa (Region 1) (first quarter of year 2014)

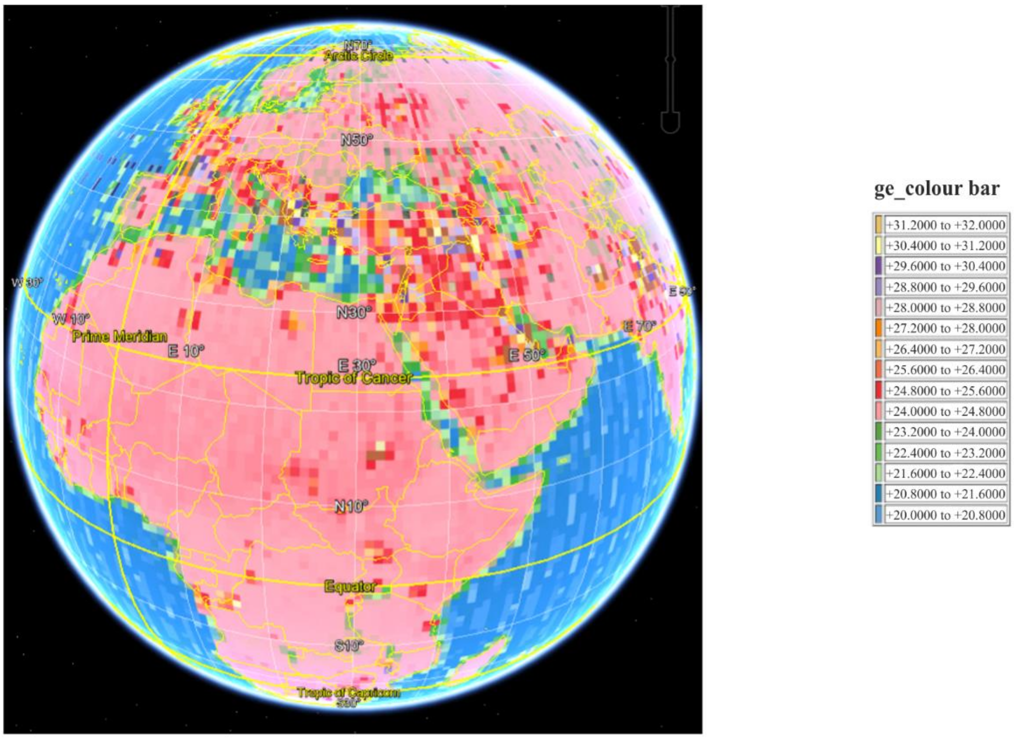

Report RS.2490-15

FIGURE 16

Map of observed BT at radiometer input for Europe and Northern Africa (Region 1) (first quarter of year 2015)

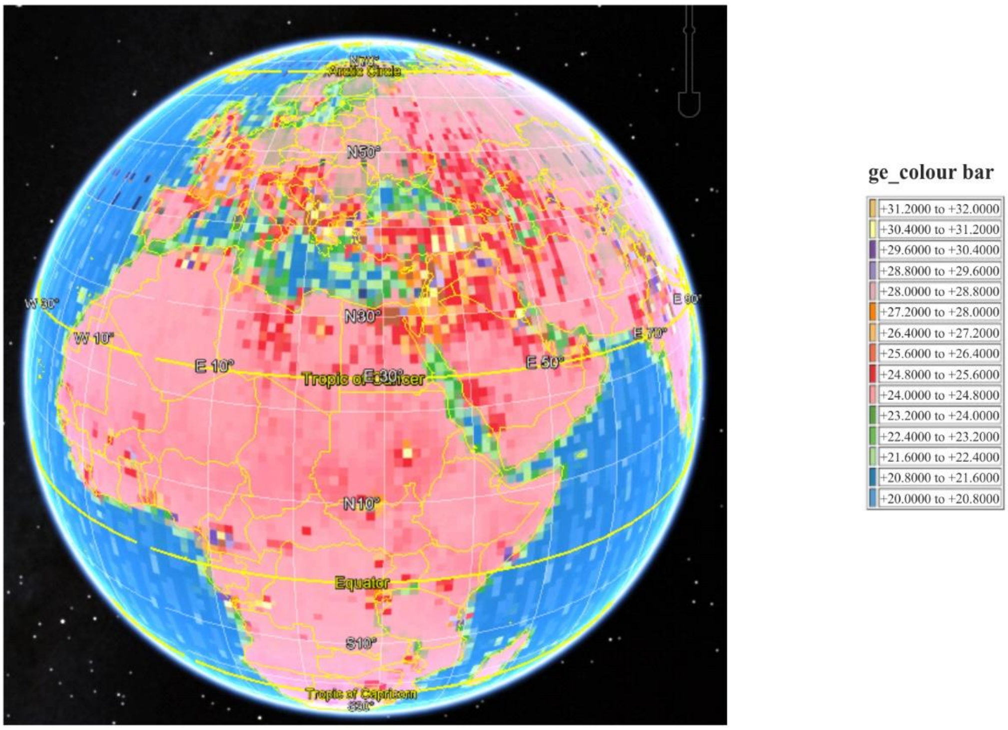

Report RS.2490-16

FIGURE 17

Map of observed BT at radiometer input for North America (Region 2) (first quarter of year 2014)

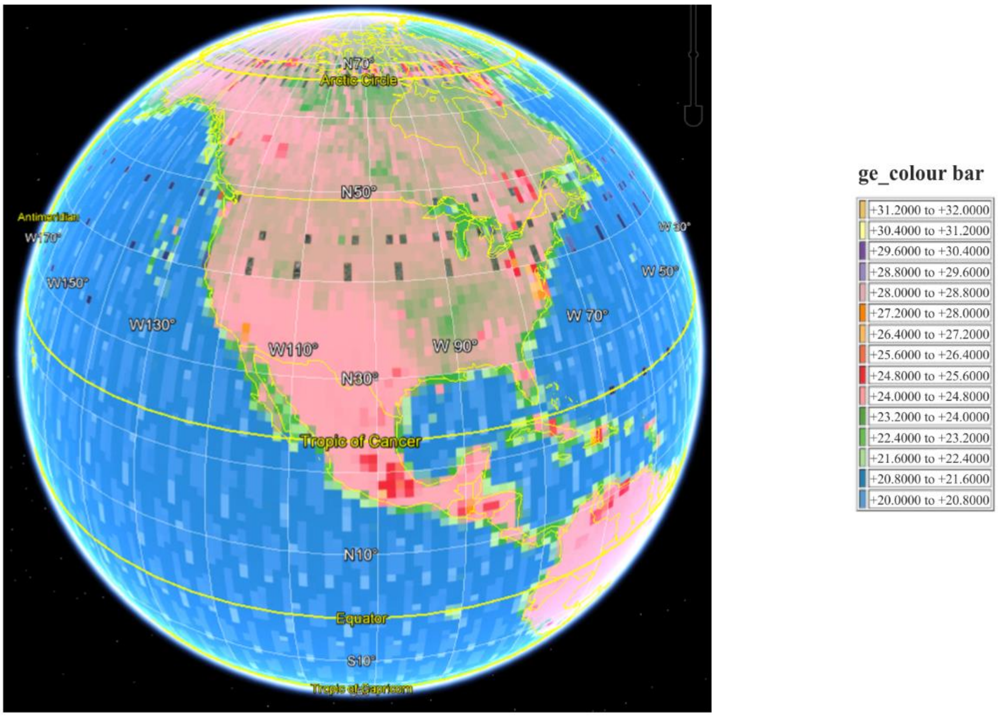

Report RS.2490-17

FIGURE 18

Map of observed BT at radiometer input for North America (Region 2) (first quarter of year 2015)

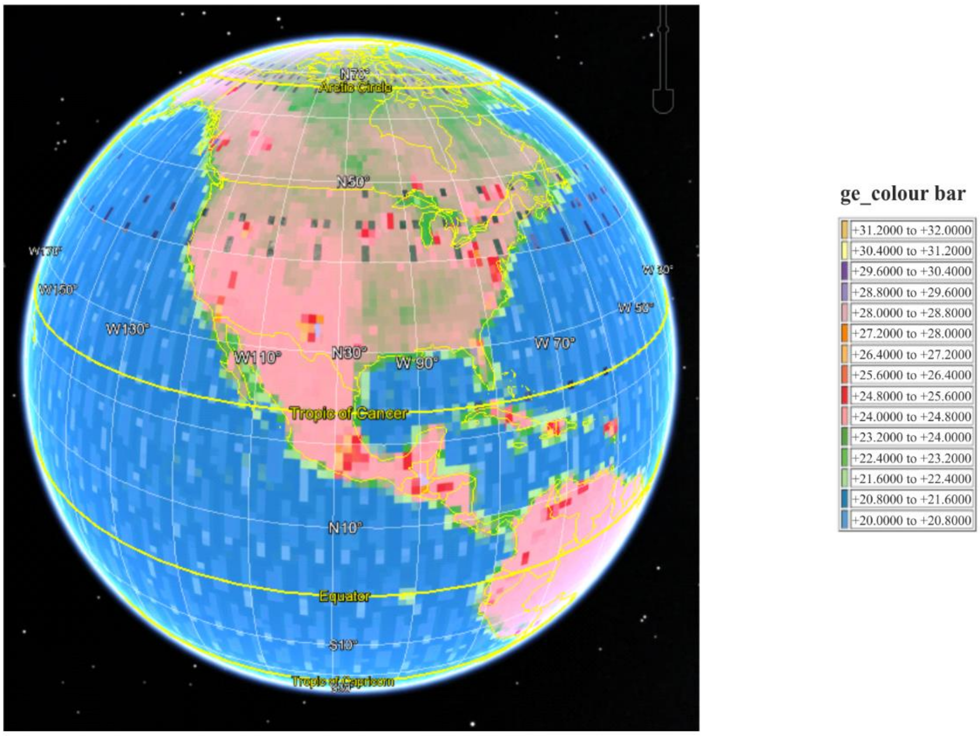

Report RS.2490-18

FIGURE 19

Map of observed BT at radiometer input for Asia (Region 3) (first quarter of year 2014)

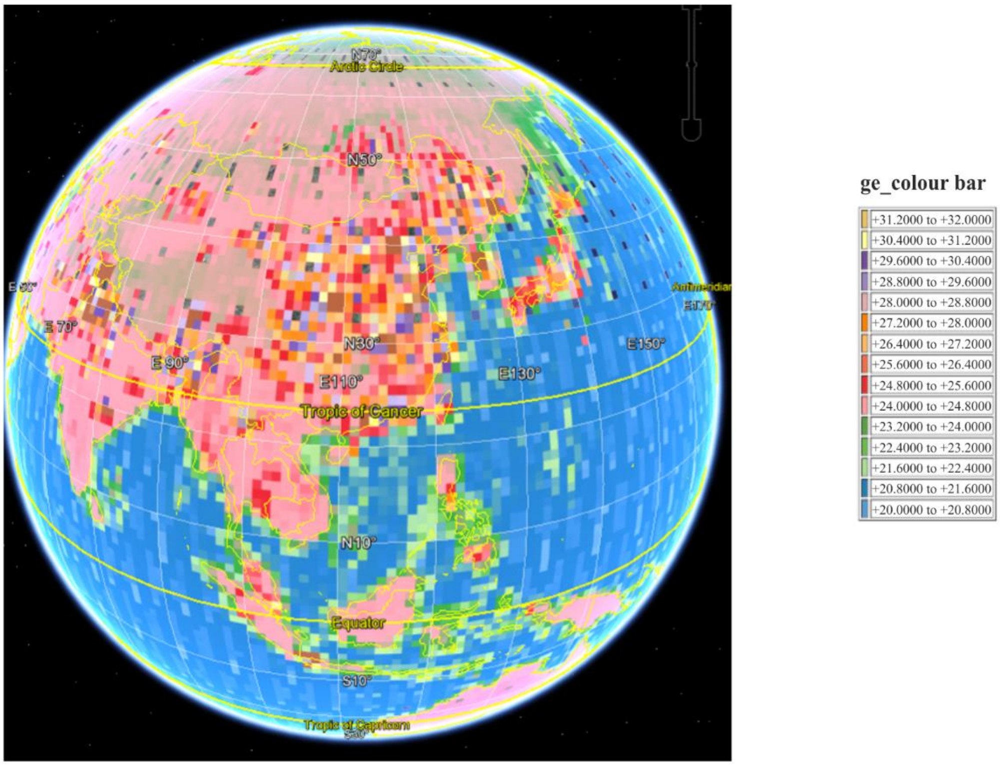

Report RS.2490-19

FIGURE 20

Map of observed BT at radiometer input for Asia (Region 3) (first quarter of year 2015)

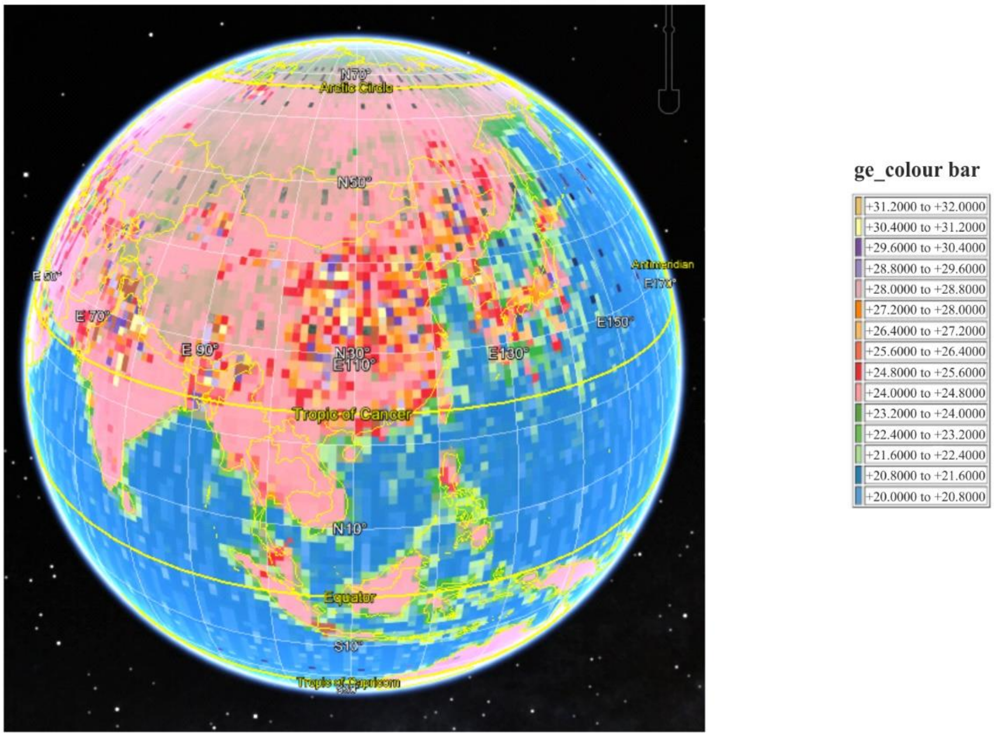

Report RS.2490-20

7 Summary

Within this Report, information has been presented on RFI as was observed globally by Aquarius L-band spaceborne active sensors operation in the EESS (active) frequency band of 1 215-1 300 MHz and Aquarius L-band spaceborne passive sensor operating in the EESS (passive) frequency band of 1 400-1 427 MHz during the January to-March 2015 time period.

Global maps of observed RFI levels in dBm were shown for the EESS (active) system Aquarius scatterometer in the frequency band 1 215-1 300 MHz. Global maps of observed BT in dB K were shown for the EESS (passive) system Aquarius radiometer in the 1 400-1 427 MHz frequency band. Instances of high RFI were shown for the Aquarius scatterometer and radiometer.

In cases where RFI sources could not be switched off, it was very important to ensure that the RFI sources were detected and flagged accordingly. RFI filtering methods are continuously improving and evolving, however low levels of RFI added to the signal caused difficulties due to the inability in distinguishing between natural and man-made radiations and which had a strong impact on the overall data quality and interpretation of the measurements.

For the case of the Aquarius scatterometer, an RFI detection and filtering algorithm had to be developed for ground data processing. Most RFI over the ocean was effectively removed, and a substantial amount of RFI was over most land areas. The global survey maps of RFI centred at 1 260 MHz, as observed during the January-to-March 2015 period, showed that certain land areas were contaminated with RFI. Fortunately, this land area RFI had no impact on Aquarius measurements to estimate sea salt salinity. However, it is not known to what degree this RFI impacted sensor measurements of soil moisture such as those obtained by SMAP.

____